Chapter 9: Thermal Performance

9.1. Introduction

The crucial parameter in designing nuclear power plants is the power produced in the core and its removal by the coolant. To that end, water at ~ 280^{o}C is circulated through the fuel assemblies and heat flows from the fuel rods to the coolant, which experiences a temperature rise as it passes through the core (see Chap.1). Since the heat is generated inside the fuel rods and flows radially-outward, temperature gradients are established within the rods, with concomitant strong influences on the mechanical properties, on the microstructure evolution under irradiation and on corrosion processes both in the fuel and in the cladding. Thus, a sound understanding of the factors governing the temperature distribution within a reactor fuel element is essential to predicting its performance during reactor exposure.

High operating temperatures lead to high thermal efficiency, but several degradation processes are accelerated with temperature. The temperature controls processes in the fuel such as: i) grain-growth; ii) densification iii) fission-product diffusion; iv) radiation damage accumulation; and v) corrosion rates on the cladding inner diameter (ID) and outer diameter (OD). Temperature *gradients* in the fuel can cause thermal stresses and fuel cracking. In the cladding, temperature gradients cause hydride formation and hydrogen redistribution.

The topic of this chapter is the thermal performance of the fuel rod, including a calculation of the temperature distribution in the fuel rod, and its change with reactor exposure. The thermal limits and accident conditions are also briefly discussed.

9.2. Fission Heat Generation

Nuclear energy is generated in light-water reactors by the fission of uranium induced by absorption of neutrons. Fission splits the uranium atom into two low-mass isotopes (the fission products), and releases two to three energetic neutrons (average energy ~ 2 MeV) as well as other particles such as betas, gammas and neutrinos. The neutrons released cause fissions in other nuclei, which releases more neutrons. This sequence constitutes the *fission chain reaction*.

9.2.1. Energy Release from fission

The overall energy release in a single fission reaction is 200 MeV, about 95% of which (190 MeV) is deposited in the fuel pellet (Sect. 20.2.1). Although every nuclide in the transuranic region can be fissioned if enough energy is imparted to it, the fission cross-section for certain *fissile* nuclides (U-233, U-235, Pu-239, Pu-241) is greatly increased if the neutron energy is close to thermal energy (~ 0.025 eV at ~ 300^{o}C). In thermal reactors (such as the light-water reactors considered in this book), reduction from the ~ 1 MeV birth energy is achieved by the passage the neutron flux through a *moderator* (water) which causes the neutrons to lose energy by successive collisions with H atoms until they are in *thermal equilibrium* with their surroundings (becoming *thermal* neutrons). Because neutrons can be lost to absorption in non-fissile materials or escape from the core, it is

necessary to enrich uranium in the U-235 isotope, so that a fission chain reaction at a constant rate (criticality) can be maintained.

In parallel with neutron-induced fission, uranium absorbs neutrons to form *transuranic* (heavier than uranium) elements.. Of chief importance among these is Pu-239, which is fissile and forms directly by neutron absorption in U-238 followed by beta decay. At the end of the fuel residence time in the reactor, up to one third of the reactor energy is produced by plutonium fission. Not all the fissile material has been consumed by the time the fuel is removed from the reactor. The remaining (and still valuable) U and Pu can be separated from the used fuel by chemical *reprocessing* and re-fabricated into mixed-oxide fuel (MOX) consisting of $(U,Pu)O_2$ (see Sect. 16.1).

This means there are various sources of heat in a reactor core: fast fission of U-238, thermal fission of U-235 and Pu-239, and the radioactive decay of fission products. The last of these is important in loss-of-coolant accident scenarios, since shutting down the fission chain reaction does not eliminate this heat source and cooling needs to be provided to avoid fuel damage (see Chap. 28).

The first step in calculating the temperature distribution in a fuel rod is specification of the rate of heat production by fission. In a fuel element at the beginning of life, the fission rate is given by

$$\dot{F} = qN_U\sigma_{f\,235}\phi_{th} \tag{9.1}$$

where $\dot{F}$ is the fission-rate density (fissions/cm^3-s), ϕ_{th} is the thermal neutron flux ($\sim 2 \times 10^{13}$ n.cm^{-2}.s^{-1}), σ_{f235} the thermal fission cross section of ^{235}U (5.5×10^{-22} cm^2 or 550 barns), q is the enrichment (0.03 – 0.05 ^{235}U /U atom) , and N_U is the uranium density in UO_2 (2.5x 10^{22} atom/cm^3). This gives a fission rate density between 0.8 and 1.3 x 10^{13} s^{-1}cm^{-3}, which is equivalent to a linear heat rate (LHR) as high as 300 W/cm for a standard fuel rod (see Eq. (9.7) and Chap. 20).

9.2.2. Fuel Burnup

The extent of fissioning of the fuel is measured by the *burnup* of which there are three definitions.

The first is the *fission density* given by

$$F = \int_0^t \dot{F}(t)dt \cong \bar{\dot{F}}t \quad [fission/cm^3] \tag{9.2}$$

where t is the exposure time, and $\bar{\dot{F}}$ is the average fission-rate density during the fuel's residence time in-reactor.

The second is *fissions per initial metal atom*, or FIMA:

$$FIMA = \frac{F}{N_U} \tag{9.3}$$

The third definition (abbreviated as bu) is the number of megawatts days of thermal energy released by a fuel initially containing one kilogram of uranium. The 190 MeV

released in each fission that is deposited in the fuel corresponds to 3.0×10^{-11} J. Thus, from Eq (20.9):

$$bu(MWd/kgU) = 887 FIMA \tag{9.4}$$

Average fuel discharge burnups have been increasing for the past two decades, now reaching over 50 MWd/kgU for PWRs and approaching that for BWRs [1]. The Nuclear Regulatory Commission (NRC) has established a burnup limit of 62.5 MWd/kgU. Current efforts to certify fuel for higher burnups are discussed in Chapter 28.

9.3. Fission Heat Removal

The thermal design of a fuel element is constrained by various limits. The difference between a limiting condition and the actual state of the fuel is termed the *margin*. The most obvious limiting conditions require operating temperatures well below the melting temperatures of the fuel (3140 K) and the cladding (2150 K). Other limiting conditions are listed in Section 9.6. In addition, the outlet coolant should be as hot as possible in order to maximize thermal efficiency (electrical energy generated to fission energy released). However, the vapor pressure of water and its corrosive effects on the fuel and primary coolant circuit limit this operating condition.

Large temperature gradients in the fuel should be avoided because of the issues mentioned in Sect. 9.1. These constraints dictate a fuel with high thermal conductivity. This is best achieved with metallic fuels, whose thermal conductivities are much higher than that of UO_2. However, metallic fuels exhibit serious dimensional instabilities under irradiation (Chap.27), while uranium dioxide is a remarkably stable matrix: it can undergo thermal cycling, withstand severe radiation damage and accommodate within its lattice the fission products and transuranic atoms produced during irradiation. Because of these features, its low thermal conductivity and associated high temperature gradients in the fuel are tolerated, although it is the performance-limiting physical property of UO_2.

9.3.1. Heat Conduction in the Fuel (see also Sect. 16.7)

95% of fission- energy is removed as heat from the fuel element by *conduction* in the geometry shown in Figure 9.1. Heat is generated in the pellet and flows radially through the fuel, the pellet-cladding gap, and the cladding proper to reach the coolant. Because the axial temperature variation is relatively gradual and there is comparatively little azimuthal temperature variation, considering only *radial* heat flow is a good approximation. The steady-state heat conduction equation is:

$$\frac{1}{r}\frac{d}{dr}\left(r\,k_F\frac{dT}{dr}\right)+Q(r)=0 \tag{9.5}$$

where T is the temperature, r the radial position in the pellet, k_F is the fuel thermal conductivity and Q is the *volumetric heat generation rate* (W/cm^3) given by

$$Q = 3.0\times10^{-11}\dot{F} \tag{9.6}$$

where 3.0×10^{-11} is the energy deposited in the fuel with each fission (about 190 MeV, Sect 20.2). Although the heat-generation rate Q varies by ~ 5% with radial position (r) because of self-shielding and other flux-gradient effects $Q(r)$ in Eq (9.5) can be approximated by the average volumetric heat generation rate, $\bar{Q}$ (W/cm^3).

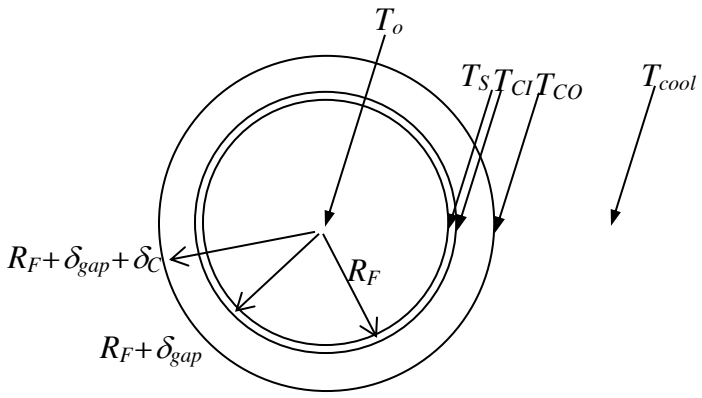

Fig. 9.1: The heat transfer geometry in a nuclear fuel rod

Another useful quantity is the *linear heat generation rate (W/cm)*, or LHR, which is the heat rate delivered per unit length of fuel:

$$LHR = \pi R_F^2 \bar{Q} \tag{9.7}$$

Where $\bar{Q}$ is the radially-averaged heat generation rate.
The boundary conditions for Eq (9.5) are:

$$T(R_F) = T_S \tag{9.8}$$

$$\left.\frac{dT}{dr}\right|_{r=0} = 0 \tag{9.9}$$

where T_S is the fuel-surface temperature.

Assuming that k_F is temperature-independent, integrating equation Eq (9.5) twice and using Eqs (9.8) and (9.9)yields the radial temperature profile in the fuel:

$$T(r) - T_S = \frac{\bar{Q} R_F^2}{4 k_F}\left(1 - \frac{r^2}{R_F^2}\right) = \frac{LHR}{4\pi k_F}\left(1 - \frac{r^2}{R_F^2}\right) \tag{9.10}$$

or

$$\frac{T(r) - T_S}{T_o - T_S} = 1 - \frac{r^2}{R_F^2} \tag{9.11}$$

where T_o is the fuel-centerline temperature. Thus a *parabolic* temperature profile is established whenever heat generation and fuel thermal conductivity are radially-constant.

From Eqs, (9.7) and (9.10) it follows that the centerline-to-surface fuel temperature difference is given by:

$$T_o - T_S = \frac{LHR}{4\pi k_F} \tag{9.12}$$

The equivalent calculations for plate and sphere geometry are given as

$$T(x) - T_S = \frac{LHR}{2\pi k_F}\left(1 - \frac{x^2}{t_F^2}\right) \text{ (plate)} \tag{9.13}$$

where in this case x is the distance from the mid-plane of the fuel and t_F is the plate fuel thickness, and

$$T(r) - T_S = \frac{LHR}{6\pi k_F}\left(1 - \frac{r^2}{R_F^2}\right) \text{ (sphere)} \tag{9.14}$$

and r is the distance from the sphere center and R_F is the radius of the sphere.

The average fuel temperature is calculated using:

$$\bar{T} = \frac{1}{\pi R_F^2}\int_0^{R_F} 2\pi r T(r)dr = 2\int_0^1 \eta T(\eta)d\eta \tag{9.15}$$

where $\eta = r/R_F$. Substituting Eq(9.11) into Eq (9.15) gives:

$$\bar{T} = \tfrac{1}{2}(T_o + T_S) \tag{9.16}$$

9.3.2. Heat Transfer Resistances beyond the fuel

The heat flux from the fuel flows through the fuel-cladding gap, through the cladding by conduction and through the hydrodynamic boundary layer into the coolant.

Heat transfer through the gap is characterized by a conductance, h_{gap}. If the gap is open,

$$h_{gap} = \frac{k_{gap}}{\delta_{gap}} \tag{9.17}$$

where δ_{gap} is the gap thickness and k_{gap} the thermal conductivity of the gas in the gap. In as-fabricated fuel rods, the gap is filled with helium at ~ 10 atm pressure. The reason for initial pressurization is to avoid drastic thermal-conductivity reduction as fission-gases such as xenon and krypton are released from the fuel (see Example #2 below). The thermal conductivities of these gases are (see Ref. [3], Eq (10.102)):

$$k_{gas} = A \times 10^{-6} T^{0.79} \quad W/cm-K \tag{9.18}$$

where A = 16 for He and A = 0.7 for Xe. A simple mixing rule is:

$$k_{gap} = k_{He}^{1-y} k_{Xe}^{y} \tag{9.19}$$

The fraction of Xe in the gas mixture is y.

Since the gap thickness is much less than the fuel radius, the *heat flux* through the gap is

$$q = \frac{LHR}{2\pi R_F} = h_{gap}(T_S - T_{CI}) \tag{9.20}$$

or

$$T_S - T_{CI} = \frac{LHR}{2\pi R_F h_{gap}} \tag{9.21}$$

where T_{CI} is the cladding inner surface (ID) temperature.

The next resistance in series is the cladding, for which an analysis similar to that for the gap yields:

$$T_{CI} - T_{CO} = \frac{(LHR)\delta_C}{2\pi(R_F + \frac{1}{2}\delta_C)k_C} \cong \frac{LHR}{2\pi R_F (k_C/\delta_C)} \tag{9.22}$$

T_{CO} is the cladding outer surface (OD) temperature, k_C is the cladding thermal conductivity and δ_C is the cladding wall thickness.

Heat transfer from the cladding outer diameter to the coolant occurs by convection:

$$T_{CO} - T_{cool} = \frac{LHR}{2\pi R_F h_{cool}} \tag{9.23}$$

where T_{cool} is the bulk coolant temperature and h_{cool} is the convective heat transfer coefficient between the cladding wall and the coolant, given for example by the Dittus-Boelter relation, equation (9.46) [2].

Adding Eqs (9.21), (9.22) and (9.23) yields:

$$T_S - T_{cool} = \frac{LHR}{2\pi R_F h} \tag{9.24}$$

where

$$\frac{1}{h} = \frac{1}{h_{gap}} + \frac{\delta_C}{k_C} + \frac{1}{h_{cool}} \tag{9.25}$$

Table 9.1. Typical Thermal properties of materials of fuel-rod and core internals for room temperature before irradiation

Material	**Density ρ (g/cm^3)**	**Specific Heat C_p (J/g-K)**	**Thermal conductivity k (W/cm-K)**	**Thermal expansion coefficient α (K^{-1})**
UO_2	10.98	0.33	0.03*	1.45×10^{-5}
Zircaloy	6.5	0.35	0.17	$5\text{-}10 \times 10^{-6}$
Steel	8.0	0.5	0.17	9.6×10^{-6}

*for equation A=23 cm.K/W, and B=0.007cm/W for UO_2.

Example 9.1: Fuel-Rod Temperature Profile

Calculate the temperature profile for a fuel rod using the following data.

T_{cool}=580 K

LHR = 200 W/cm

h_{cool} =2.5 W/cm^2- K

Fuel pellet radius R_F =0.5 cm

Cladding thickness δ_C= 0.06 cm

Gap width δ_{gap}= 30 μm

From Eq (9.23) and h_{cool}: $T_{CO} - T_{cool}$ = 21 K

From Eq (9.22): $T_{CI} - T_{CO}$ = 17 K

From Eq(9.18): k_{gas} = 0.0025 W/cm-K (He)

From Eq (9.17): h_{gap} = 0.71 W/cm^2-K (with He)

From Eq (9.21): $T_S - T_{CI}$ = 90 K

From Eq (9.12): $T_o - T_S$ = 530 K

T_o = 580 + 21 + 23 + 90 + 530 = 1244 K (=971 C)

The calculated profile is shown as the dashed curve in Fig. 9.2. It is clear that the greatest contributor to the increase in centerline temperature is the temperature rise in the fuel, but the gap can have a significant impact as well - in this case a temperature drop of 90 K.

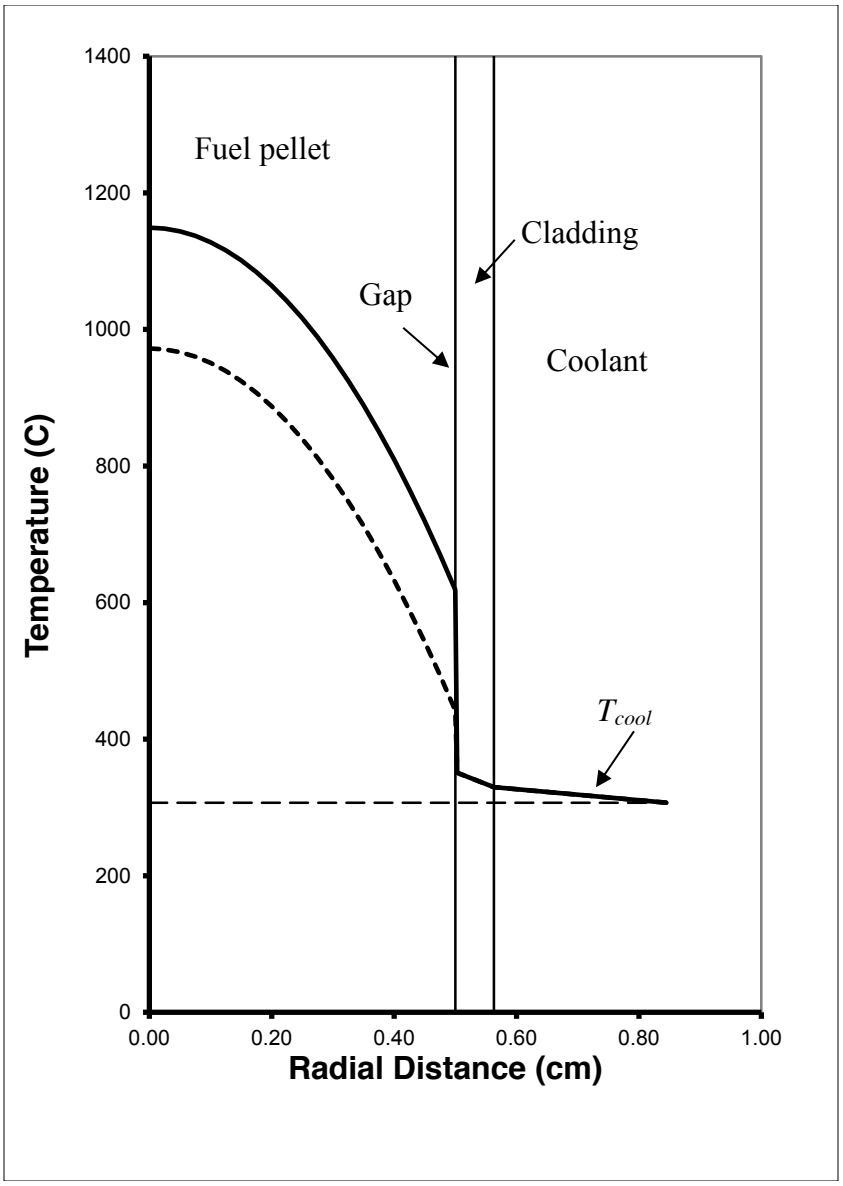

Figure 9.2 Temperature Profile in a fuel rod (see examples 9.1 and 9.2). The dotted line represents the bulk coolant temperature, while the dashed and continuous temperature profiles represent the two cases calculated in examples 9.1 and 9.2.

The effect of the gap worsens with increasing burnup, since xenon gas released into the fuel-cladding gap degrades its thermal conductivity. The result is shown in Example #2. in which all other parameters are the same as in Example # 1, while substituting a fraction of xenon for helium.

Example 9.2: Correction to Fuel-Rod temperatures: Calculate the temperature profile when Xe is released.
Effect of 6% fission-gas release from fuel after 3% burnup of uranium;
fuel porosity = 5%; length of fuel stack = 300 cm; plenum length = 20 cm;

moles UO_2 = $\frac{\pi(0.5)^2(300)(0.95)(10.98)}{270} = 9.1$

gas space in rod = $\pi(0.5)^2(20) + 2\pi(0.5)(0.008)(300) = 15.7 + 7.5 = 23.2$ cm^3

plenum initial gap

Fuel-rod fabrication: 80 μm initial gap thickness; helium fill gas: 373 K; 10 atm

moles He = $\frac{(10)(23.2)}{(82)(373)} = 7.6\times10^{-3}$

Xe produced = 9.1×0.03×0.25 = 0.068 moles (Xe fission yield = 0.25)

Xe released = 0.068×0.06 = 4.1×10^{-3} moles

y =gap-gas Xe fraction = $\frac{4.1}{7.6+4.1} = 0.35$

assume temperature of gas in gap ~ 623 K

From Eq (9.18): $k_{He} = 16\times10^{-6}(623)^{0.79} = 2.1\times10^{-3}$; $k_{Xe} = 0.7\times10^{-6}(623)^{0.79} = 9.6\text{x}10^{-5}$ W/cm-K

From Eq (9.19): $k_{gap} = (2.1\times10^{-3})^{0.65}(9.6\times10^{-5})^{0.35} = 7.1\times10^{-4}$ W/cm-K (a factor of 3 lower than pure He)

$h_{gap} = \frac{7.1\times10^{-4}}{30\times10^{-4}} = 0.24\frac{W}{cm^2K}$

From Eq (9.21): $T_S - T_{CI} = 267$ K

The Xe in the gap increases ΔT_{gap} by 177 K

If during fabrication of the fuel rod the gap had contained 1 atm He instead of 10 atm, the gap gas composition would have been 84% Xe. k_{gap} would have been reduced to 1.57×10^{-4} W/cm-K and ΔT_{gap} would have been an unacceptable 1215 K.

.

9.3.3. Gap Closure on initial heatup

There are two causes of fuel-cladding gap closure at startup: thermal expansion and fuel cracking. Here we deal in detail only with the first.

The change in gap width upon fuel and cladding expansion is given by

$$\Delta\delta_{gap} = \delta_{gap} - \delta^{o}_{gap} = \Delta\bar{R}_C - \Delta R_F \tag{9.26}$$

The superscript ^{o} indicates an as-fabricated value. $\Delta\bar{R}_C$ is the change in mean cladding radius and ΔR_F is the change in fuel radius, both as a result of the temperature increase on startup in the reactor. The radial strain of the fuel in a parabolic temperature profile is given by (Prob 9.1):

$$\frac{\Delta R_F}{R_F} = \alpha_F(\bar{T}_F - T_{fab}) \tag{9.27}$$

where the average fuel rod temperature $\bar{T}_F$ is calculated from Eq (9.14). T_{fab} is the fuel fabrication temperature and α_F is the coefficient of thermal expansion of UO_2. The corresponding increase for the cladding is approximately equal to

$$\frac{\Delta R_c}{\bar{R}_c} = \alpha_c(\bar{T}_c - T_{fab}) \tag{9.28}$$

An approximation to the change in gap width upon heating is given by:

$$\Delta\delta_{gap} = \delta^{hot}_{gap} - \delta^{fab}_{gap} = \bar{R}^{o}_{C}\alpha_C(\bar{T}_C - T_{fab}) - R^{o}_{F}\alpha_F(\bar{T}_F - T_{fab}) \tag{9.29}$$

The error introduced in this equation is the estimation of the mean fuel temperature, $\bar{T}_F$, which is a function of the gap thickness, which is the unknown.

Example 9.3 Gap closure on initial heatup

For this example LHR = 150 W/cm and $\delta^{o}_{gap} = 80\ \mu m$; $T_{fab} = 373$ K

note: cannot assume $\delta_{gap} = 30\ \mu m$, as was done in Example 9.1. What remains from this example are: $T_{CO} = 580 + 21 = 601$ K; $T_{CI} = T_{CO} + 17 = 618$ K; $\bar{T}_C = 609$ K, $\delta_C = 0.1$ cm (note that a different value of cladding thickness is used here).

$R^{o}_{F} = 0.5$ cm $\quad \bar{R}^{o}_{C} = 0.5 + 0.008 + \frac{1}{2} \times 0.1 = 0.558$ cm

from Eq(9.29): $\bar{R}_C = \bar{R}^{o}_{C}\left[1 + \alpha_C(\bar{T}_C - T_{fab})\right] = 0.559$ cm

Because the temperature profile depends on the dimensions and vice versa, an iterative solution is required:

Trial-and-error solution:

iteration	1	2	3	4	5	6	Ex. #1
Guess of T_S (K)	680	690	700	710	720	**715**	**678**
$T_o = T_S + LHR/(4\pi k_F)$	1078	1088	1098	1108	1118	**1113**	**1076**
$\overline{T}_F = \frac{1}{2}(T_o + T_S)$	879	889	899	909	919	**914**	**877**
$R_F = R_F^o[1 + \alpha_F(\overline{T}_F - T_{fab})]$	0.5036	0.5037	0.5038	0.5039	0.5040	**0.5040**	**0.5000**
$\delta_{gap} = \overline{R}_C - \frac{1}{2}\delta_C - R_F$ (μm)	54	53	52	51	50	**50**	**30**
$h_{gap} = k_{He}/\delta_{gap}$	0.469	0.475	0.482	0.489	0.496	**0.493**	**0.8**
$T_S = T_{CI} + LHR/(2\pi R_F^o h_{gap})$	720	718	717	716	714	**715**	**678**

The sixth column shows the converged results and the last column contains the results of Example 9.1 in which δ_{gap} = 30 μm was arbitrarily used. Accounting for thermal expansion of fuel and cladding (and for specification of the size of the as-fabricated gap) increases the calculated at-power gap thickness to 50 μm. This results in a larger temperature drop over the gap and an increase in the fuel centerline temperature from 1076 K to 1113 K. The very significant effect of the 20 μm increase in gap thickness is due to the poor thermal conductivity of helium .

Using the value of 877 K obtained in Example 9.1 and the as-fabricated gap thickness of 80 μm, the hot-gap size from Eq (9.29) is 54 μm. This is only 4 μm larger than the value calculated by the trial-and-error method shown in the above table. Unless high accuracy is required, the combination of Eq (9.29) and the type of computation employed in Example 9.1 is generally sufficient for most purposes.

The tangential stress in the fuel pellet subject to a radially-constant heat generation rate is:

$$\sigma_\theta = -\frac{\alpha_F E_F (LHR)}{16\pi(1-\nu_F)k_F}\left(1 - 3\frac{r^2}{R_F^2}\right) \tag{9.30}$$

E_F is the elastic constant of UO_2 and ν_F its Poisson ratio. The outer 40% of the pellet is under tensile stress (azimuthal) that for usual LHRs, exceeds the fracture stress. A typical cracking pattern is shown in Fig. 9.3 [3].

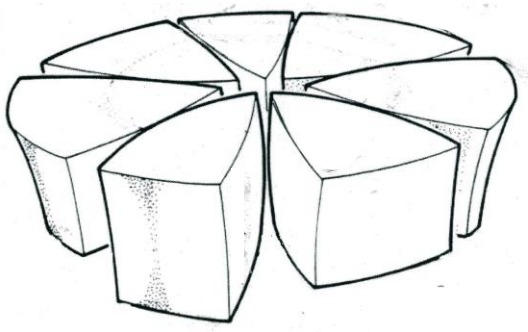

Fig. 9.3 Cracks in fuel pellet due to the stresses induced by the temperature gradient

Additional features of the gap conductance, particularly for a closed gap, can be found in Sect. 10.4.5 of Ref. 3.

9.4. Axial Temperature Profile

The calculations in Sect. 9.3 were performed for *radial* transfer of heat. Because of temperature differences along the length of the fuel rod, heat is also transferred in the *axial* direction.

The axial variation of the linear heat rate distribution can be written as:

$$LHR\left(\frac{z}{Z_o}\right) = LHR^o \cos\left[\frac{\pi}{2\gamma}\left(\frac{z}{Z_o} - 1\right)\right] = LHR^o\, F\left(\frac{z}{Z_o}\right) \tag{9.31}$$

where z is the axial distance, LHR^o is the centerline linear heat rate ($z/Z_o=1$), and $\gamma = (Z_{ex}+Z_o)/Z_o$ represents the ratio of the axial extrapolation distance of the neutron flux to the fuel-rod half-height. A typical value is $\gamma = 1.3$. Angles are expressed in radians.

Because of the above variation of the LHR and the increasing temperature of the coolant as it passes through the core, the fuel supports an axial temperature profile. The left-hand diagram of Fig. 9.4 shows a square array of fuel rods with the flow area per rod inside the square. This diagram is modified in the center to a form suitable for computation by creating an equivalent *circular* area around each rod. The right-hand sketch shows the rod and associated coolant flow in the z direction. The energy balance of the circular slice dz is:

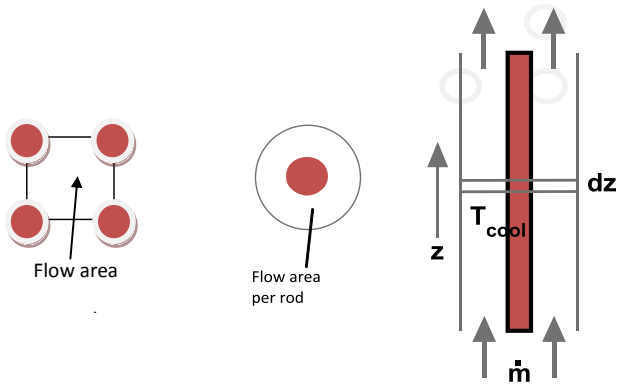

Fig. 9.4 Upflow of coolant per fuel rod

$$\dot{m} C_{PW} \frac{dT_{cool}}{dz} = LHR\left(\frac{z}{Z_o}\right) \tag{9.32}$$

Integrating from the core entry (z = 0) to height z:

$$\dot{m}C_{PW}(T_{cool}-T_{cool}^{in})=Z_o\int_0^{z/Z_o} LHR\left(\frac{z}{Z_o}\right)d\left(\frac{z}{Z_o}\right) \tag{9.33}$$

where $\dot{m}$ is the mass flow rate per fuel rod (kg/s-rod), C_{PW} is the coolant specific heat (J/kg-K) and T_{cool}^{in} is the inlet coolant temperature. Substituting Eq (9.31):

$$\dot{m}C_{PW}(T_{cool}-T_{cool}^{in})=Z_o\times LHR^o\int_0^{z/Z_o} F\left(\frac{z}{Z_o}\right)d\left(\frac{z}{Z_o}\right) \tag{9.34}$$

$$T_{cool}-T_{cool}^{in}=\frac{1}{1.2}\frac{Z_o\times LHR^o}{\dot{m}C_{PW}}\left\{\sin(1.2)+\sin\left[1.2\left(\frac{z}{Z_o}-1\right)\right]\right\} \tag{9.35}$$

As expected the highest temperature occurs at the core outlet ($z/Z_o = 2$). However, the fuel centerline temperature reaches its maximum *above* the core midplane, as shown in the following example.

Example 9.4 Location of the maximum fuel temperature

What is the maximum fuel temperature and at what elevation does it occur? Use the method and parameters of Example 9.1 except for T_{cool}, which is now given by Eq (9.35). The LHR given in Example 9.1 is that at the core midplane ($z/Z_o = 1$). Assume a gap width of 30 μm at all elevations.

$\dot{m} = 0.25$ kg/s-rod; $Z_o = 150$ cm; LHR(1) = 150 W/cm; $C_{PW} = 4200$ J/kg-K $T_{cool}^{in} = 570$ K

Figure 9.5 shows the axial variations of the coolant temperature (bottom) and the centerline fuel temperature (top). Because of the relatively modest coolant temperature rise, the tilt of the centerline fuel temperature towards the top of the core is barely visible. The high fuel temperatures are restricted to the middle 1/4 of the core.

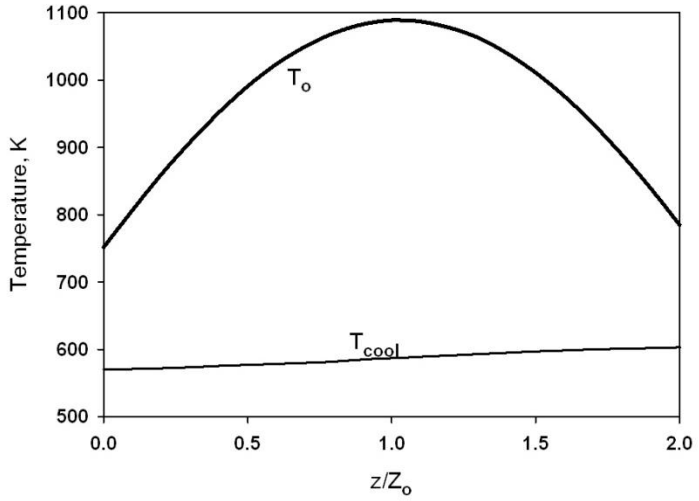

Fig. 9.5 Axial temperature distributions

9.5. Thermal Conductivity

The heat conduction equations derived above apply only when the thermal conductivity is constant (does not depend on temperature, chemistry or fuel microstructure). This section discusses the thermal conductivity of the fuel rod constituent materials, (especially the fuel), their variation with temperature, composition and burnup and the methods used to take these variations into account. In as-fabricated fuel the thermal conductivity depends on many parameters, as discussed in the following sub-sections. The cladding's resistance to heat transfer in the radial direction is most strongly affected by the formation of the ZrO_2 (or CRUD) on the outer cladding surface (Chaps. 20 and 22).

Knowledge of the thermal conductivity of the fuel, gap and cladding is essential to determining the temperature distribution and transient thermal response of the fuel rod. The thermal conductivity of the fuel also determines the amount of stored heat in the fuel which is a consequence of the large gradients that have to be established to sustain heat flow at steady state.

9.5.1. Thermal Conductivity in Porous Oxide

When uranium dioxide is fabricated into pellets, sintering conditions (Sect. 16.1) can be controlled so that the pores initially present are partially eliminated, resulting in a solid with 94 – 96% of the theoretical density of UO_2 (10.95 g/cm^3). The presence of the pores provides free space to accommodate fission gases, thus reducing swelling. However, porosity diminishes the thermal conductivity of the pellet. During irradiation, additional porosity develops in the form of fission-gas-filled bubbles (Chap. 20).

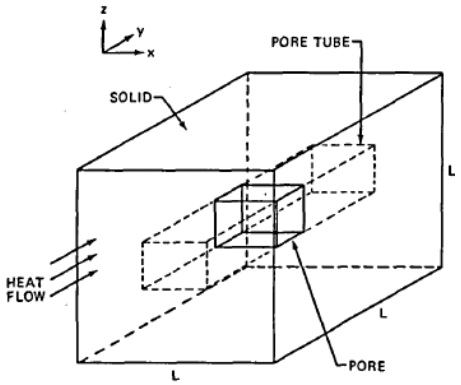

Figure 9.6. Geometry for analysis of effect of pores on thermal conductivity [4]

Consider a homogenous distribution of cube-shaped pores in which a "unit cell" consists of the pore and its associated volume, as shown in Figure 9.6. Two pathways exist for heat flow in the y direction: through the "pore tube", or through the solid surrounding the pore tube. On the latter route, the thermal conductivity is that of fully-dense UO_2. Heat flow through the pore tube is governed by the thermal conductivity of a composite of void space and solid. The pore tube and the surrounding solid are *parallel thermal resistances*, so the effective thermal conductivity of the unit cell (i.e., of the fuel) is:

$$k_F = (1-f)k_{ox} + f\,k_{poretube} \tag{9.36}$$

where *f* is the fraction of cross sectional area perpendicular to heat flow occupied by the pore tube and k_{ox} is the thermal conductivity of fully-dense UO_2. $k_{pore\ tube}$ represent the *series thermal resistances* of oxide and the pore, so:

$$\frac{1}{k_{poretube}} = \frac{g}{k_{pore}} + \frac{1-g}{k_{ox}} \tag{9.37}$$

Where *g* is the fraction of the pore tube occupied by the pore. Eliminating $k_{pore\ tube}$ between these two equations yields

$$\frac{k_F}{k_{ox}} = \frac{1+(\gamma-1)(1-f)\,g}{1+(\gamma-1)g} \tag{9.38}$$

The right-hand term is a correction factor on the thermal conductivity of 100%-dense UO_2. It depends on the geometry of the pore/solid unit cell (via f and g) and the ratio of the thermal conductivities of the oxide and the gas in the pore $\gamma = k_{ox}/k_{pore}$. If either *f* or *g* is zero, the correction factor is unity. If $\gamma = \infty$, the correction factor is *1 – f*, or no heat flows through the pore tube.

The porosity of the fuel is [Ref. [3], Eq (10.35)] :

$$P = fg \tag{9.39}$$

and if the pore is a cube:

$$f = P^{2/3}\ and\ g = P^{1/3} \tag{9.40}$$

In terms of the porosity, Eq (9.38) becomes:

$$\frac{k_F}{k_{ox}} = \frac{1+(\gamma-1)(1-P^{2/3})P^{1/3}}{1+(\gamma-1)P^{1/3}} \tag{9.41}$$

In the limit of large γ (actually $(\gamma - 1)P^{1/3} >> 1$), the correction factor is

$$\frac{k_F}{k_{ox}} = 1 - P^{2/3} \tag{9.42}$$

Example 9.5 Fuel thermal conductivity reduction due to porosity

Compare the thermal-conductivity reduction factors from Eqs (9.32a) and (9.32b) for the following parameters:

- in as-fabricated fuel P = 0.05 (5%)
- the pores are filled with a mixture of 65% helium and 35% xenon - $k_{pore} \cong 8\times10^{-4}$ W/cm-K. The UO_2 thermal conductivity is $k_{ox} \cong 0.03$ W/cm-K, so $\gamma \cong 36$.
-

Substituting these values into Eq (9.41) gives $k_F/k_{ox} = 0.87$;

That is, a 13% reduction in effective thermal conductivity relative to that of the solid UO_2. This is

close to the maximum reduction for this porosity that would be obtained if no heat flowed through the pore tube, which from Eq (9.42), $k_F/k_{ox} = 0.86$.

9.5.2.Thermal Conductivity Variation with Temperature

The integration of Eq (9.5) was performed assuming the thermal conductivity to be independent of the radial position *r*. In fact the thermal conductivity of UO_2 varies significantly with temperature, which in turn varies markedly with radial position. Rather than a constant, a typical temperature-dependent thermal conductivity is (Sect. 16.7.2):

$$k_{ox} = \frac{1}{A + BT} \tag{9.43}$$

where:

$$A = 3.6 + 200\times FIMA \ \text{ cm-K/W} \ \text{ and } B = 0.022 \text{ cm/W}$$

Equation (9.43) is a well-known empirical fit of thermal-conductivity data, is often referred to as the *Halden equation* after the Norwegian laboratory where this data was generated. Neglecting porosity ($k_F \sim k_{ox}$) the temperatures at the fuel centerline and fuel surface are related by: (see Prob. 9.2):

$$\frac{1}{B}\ln\left(\frac{A + BT_o}{A + BT_S}\right) = \frac{LHR}{4\pi} \tag{9.44}$$

Numerous correlations of k_{ox} have been prepared by Baron [5] which, in addition to temperature and porosity dependences, include the effects of plutonium and gadolinium (Fig. 9.7).

To account for the dependence of thermal conductivity on temperature, stoichiometry and plutonium content, the heat conduction equation would need to be solved with k_{ox} as a function of these variables using one of the correlations in Fig. 9.7. This is normally done by numerical methods.

Example: Account for the temperature effect on k_F according to Eq (9.44) with the A and B values given in table 9.1.
From the results of Example #1, $T_S = 714$ K.

Using Eq(9.44): $\exp\left(\frac{B\times LHR}{4\pi}\right) = \exp\left(\frac{7\times10^{-3}\times 200}{4\pi}\right) = 1.12$

$A + BT_S = 23 + (7\times10^{-3})(714) = 28$; $T_o = [(28)(1.12) - 23]/(7\times10^{-3}) = 1185$ K=917 C
This is not too far from the T_o calculated in Example 9.1. The agreement is fortuitous because a constant $k_F = 0.03$ W/cm-K used in Example # 9.1 is only a very rough average.

In addition to variations in fuel thermal conductivity, the thermal conductivity of the cladding is degraded by the oxide layer formed by waterside corrosion (Chap. 22) and also by CRUD deposits (Chap. 20).

The slight upturn in k_{ox} above 2000 K is due to electronic conduction, the main heat transport mechanism in metals. As in all ceramics, the Gibbs energy of free-electron formation in UO_2 (E_f^{el}) is large, which accounts for the very high-temperature onset of this contribution (i.e., $\exp(-E_f^{el} / k_B T)$) .

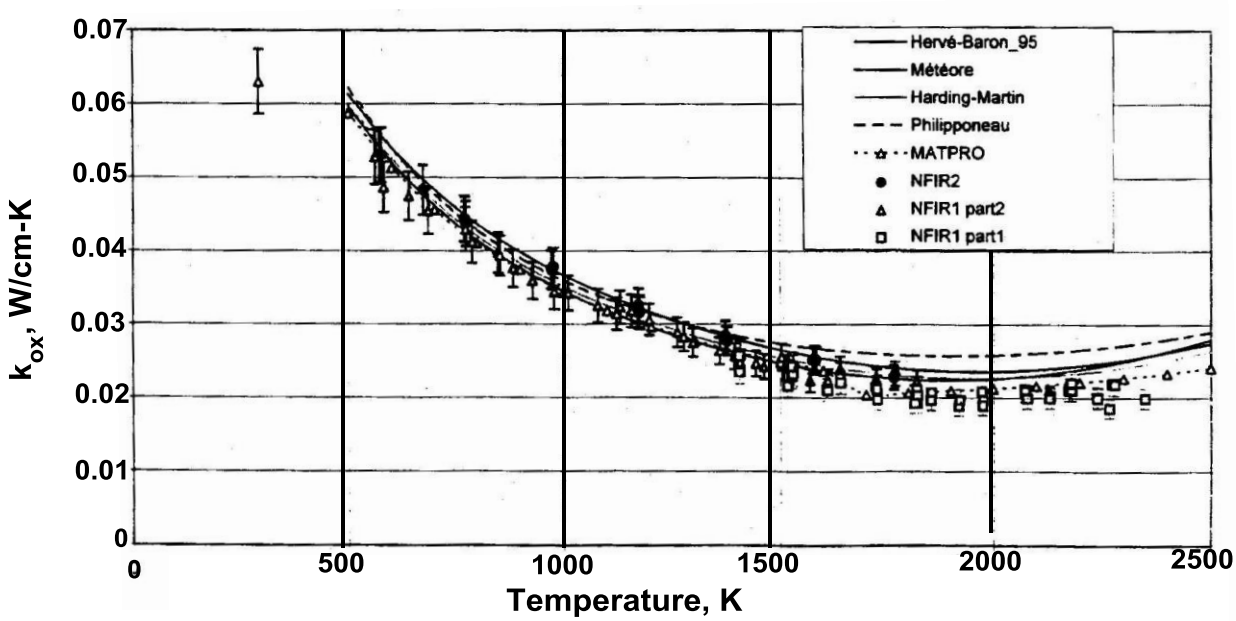

Fig. 9.7 Comparison of thermal conductivity of 95%-dense UO_2 with correlations (after ref. [5])

9.6. Thermal Margins and Operating Limits

A nuclear reactor is different from conventional power plants in one important way: the central safety tenet in nuclear power plant operation is avoidance of fuel damage and attendant release of fission products. An important safety goal is to minimization of the consequences of postulated design-basis accidents. Thus, thermal limits are prescribed both for normal operation and for accident situations, with the overall goal of avoiding fuel damage. We discuss operational limits in this section and accident limits in the next. Comprehensive reviews of these limits can be found in Ref. 5 and Chap. 28..

The operational limits provide an envelope of conditions under which fuel failure should not occur. These are linear heat rate (LHR) limits (related to departure from nucleate boiling), centerline fuel temperature limit (to avoid fuel melting) and pellet-cladding mechanical interaction (PCMI) to avoid cladding failure.

To avoid fuel damage the operational constraints are on maximum temperatures (fuel-centerline) rather than on the average rod temperature. Because the neutron flux and coolant temperature vary axially and radially through the core, so do the fuel-rod temperatures.

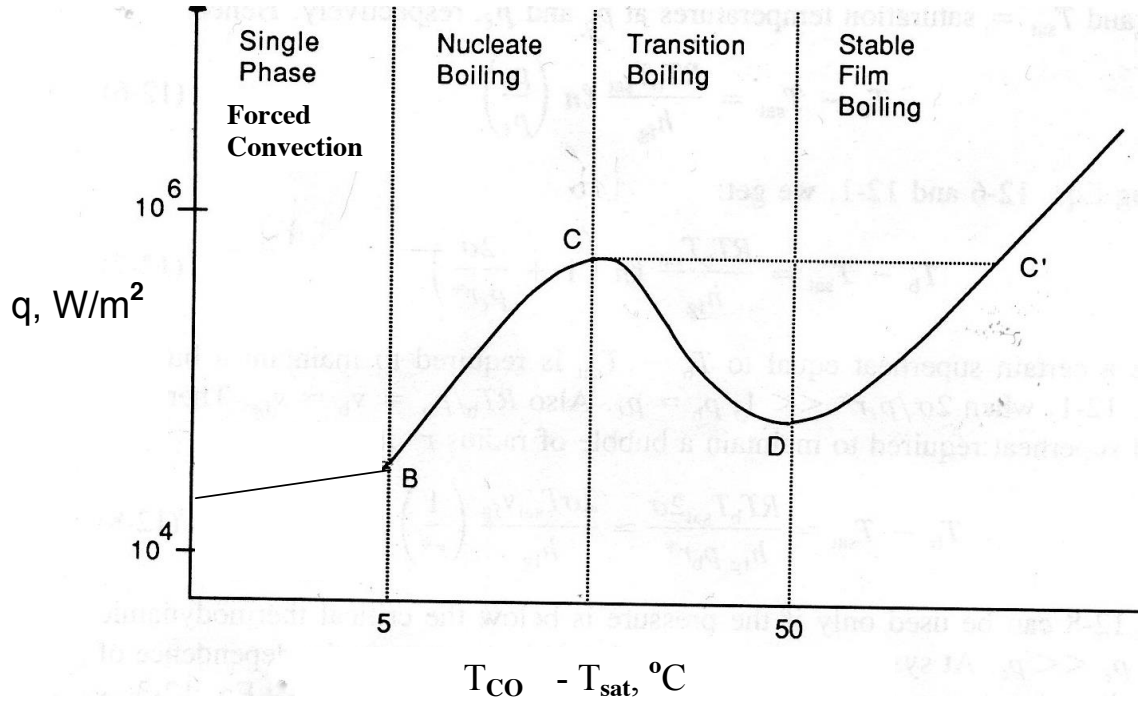

Fig. 9.8. Schematic of boiling curve in a LWR

9.6.1. Critical heat flux

As the outer skin temperature from a heated fuel rod immersed in a constant temperature liquid increases, the mode of heat transfer changes. The *boiling curve* can be determined from an experiment in pool boiling, in which the outer diameter rod temperature is gradually increased and the heat flux to the liquid is measured. Figure 9.8 shows a plot of the log of the heat flux versus the temperature difference between the rod and the bulk liquid temperature. Four forms of heat transfer can be discerned.

In the single-phase mode of heat transfer, a flux q is driven by the temperature difference between the cladding outer diameter, T_{CO}, and the bulk coolant at T_{sat}:

$$q = h\left(T_{CO} - T_{sat}\right) \tag{9.45}$$

The heat-transfer coefficient *h* that is most commonly employed for single-phase liquid is given by the Dittus-Boelter equation:

$$hd_{eq} / k_{cool} = 0.023\,\mathrm{Re}^{0.8}\,\mathrm{Pr}^{0.4} \tag{9.46}$$

where d_{eq} is the equivalent diameter of the flow channel, k_{cool} is the thermal conductivity of the coolant and Re and Pr are the Reynolds and Prandtl numbers, respectively.

One of the main concerns for fuel rods is that the linear heat flux becomes so high that *dryout* occurs. Figure 9.8. shows the rise of the outer cladding temperature T_{CO} as the heat flux q from the fuel to the coolant increases. At point B, the onset of *nucleate boiling* provides greater mixing and heat transfer to the coolant.

As the temperature of the cladding outer diameter increases beyond point B, so too does the bubble concentration in the fluid near the wall. At a critical point (C) the bubbles coalesce and a continuous film of steam is formed. Beyond point C in Fig. 9.8, the rod is blanketed by steam and the heat flux is severely decreased as the heat transfer coefficient from cladding to steam is much lower than that of cladding to water.

When a second phase is present the mechanism of heat transfer from the cladding outer surface to the bulk coolant is more complex than the mechanism that drives the heat flux in single-phase water.

The abcissa of Fig. 9.8 is $T_{CO} - T_{cool} = (T_{CO} - T_{sat}) + (T_{sat} - T_{cool})$ that because the boiling curves in depend upon the *difference* between the wall temperature and the saturation temperature not the bulk coolant temperature. The two temperature-driving forces differ by $(T_{sat} - T_{cool})$. If the system pressure is fixed, so is T_{sat}, but T_{cool} ranges from 553 K to 593 K (280°C to 320°C). In a PWR, T_{sat} = 615 K (342°C). A typical cladding OD temperature is $T_{CO} \sim 633$ K (360°C).

Nucleate boiling begins at point B (although the transition is not as distinct as shown in the figure). A typical nucleate-boiling empirical correlation applicable to PWR conditions is:

$$q\left(W / m^2\right) = 6\left(T_{CO} - T_{sat}\right)^4 \tag{9.47}$$

The temperature is in Kelvin.

Point C is known as the *critical heat flux* (CHF). In PWRs this point is identified as the *departure from nucleate boiling* (DNB). At this point, nucleate boiling turns into very-much-less-efficient *film boiling*. Above point C, the bubble nucleation rate becomes high enough that a continuous vapor film forms at the surface. When this condition is reached, the wall temperature increases precipitously, typically above 1100 K, and cladding failure is certain. To avoid reaching the critical heat flux, *thermal margins* are established. The DNBR (departure from nucleate boiling ratio) is the ratio of the heat flux that causes dryout (CHF) to the actual heat flux. Th. e DNBR scales with the incidence of fuel damage when these margins are obtained by calculations [6]. In an operating nuclear power plant it is necessary to demonstrate, by calculation and statistical analysis,

that the minimum DNBR for the hottest channel (Fig. 9.9) is larger than 1.15-1.3, a margin of 15 to 30%. Above point D the

By this definition, the DNBR is a useful measure of how close a dangerous situation is approached during normal operation.

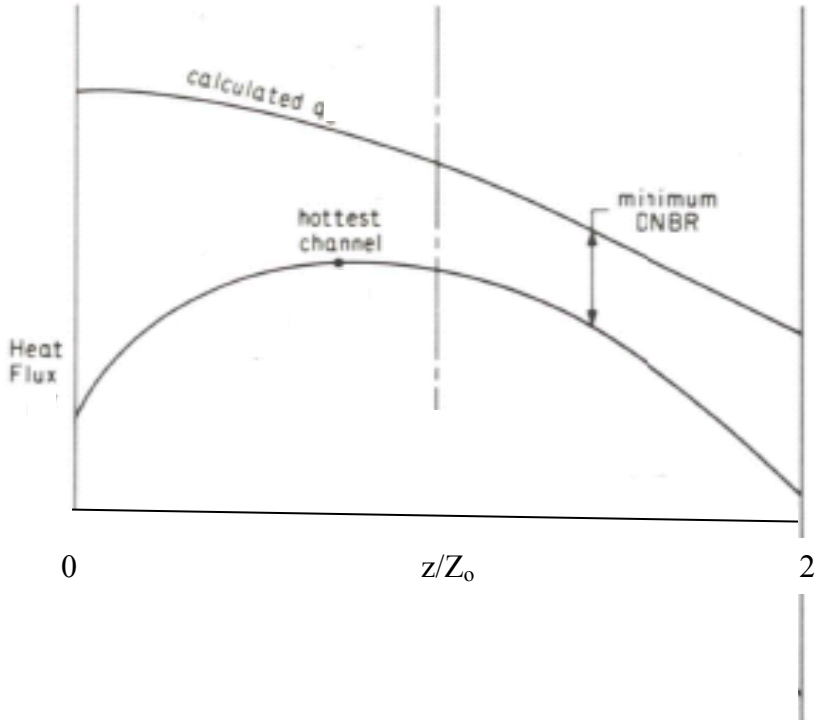

Fig. 9.9. Departure from nucleate boiling limits

The mechanism above is prevalent in PWRs, in which a majority of the liquid phase is present where bubbles are generated. In the case of a BWR in which a significant amount of vapor already exists in the flow (higher quality) an annular flow (liquid film close to the wall with a high density of bubbles) may form. A *dryout* condition can then occur as a combination of droplet entrainment and evaporation takes place, at which point the flow becomes vapor with entrained droplets. The heat transfer then decreases abruptly and a *critical heat flux* condition is again reached, this time by a dryout mechanism.

A more complete description of these phenomena can be found in [7].

9.6.2. Pellet-Cladding Mechanical Interaction

Early reports of fuel failures by pellet-cladding mechanical interaction **(PCMI)** first appeared in the 1960s. If the linear heat rate is suddenly increased, the pellet-cladding

gap closes and the fuel mechanically loads the cladding. If the resulting tensile stress in the cladding is high enough, failure can occur. This frequently occurs in fuel rods adjacent to a recently- withdrawn control rod, which causes a sudden LHR increase. The PCMI mechanism is exacerbated when the fuel is cracked or when there is missing chip on the fuel surface, which tends to localize the deformation in the cladding. With longer exposure the cladding becomes increasingly brittle, so that failure occurs at a smaller imposed strain. Chapter 23 discusses fuel failures under these conditions.

Localized PCMI can be avoided by eliminating "hourglassing" of the fuel pellet during transients by proper chamfering during fabrication. PCMI is most severe during high ramp rates because the fuel does not have time to relieve internal stresses by creep.

Pellet-cladding mechanical interaction can cause cracks to propagate from the inner diameter, assisted by the presence of fission gases (iodine assisted stress corrosion cracking, discussed in Chapters 23 and 26.Cladding with greater PCMI-resistance than standard Zircaloy has also been investigated. Softer materials are more resistant to the crack propagation which results in failure during PCMI. Duplex cladding consisting of co-extruded Zircaloy-2 and an inner (barrier) layer of (softer) Zr [8][8][8][7]. enhances PCMI resistance [7] . Essentially all BWR cladding uses some form of Zr-barrier cladding.

9.7 Limits for Accident Conditions

In light-water reactors the accidents with the greatest potential for fuel damage are those (i) producing excessive power (as in a reactivity initiated accident (RIA), or (ii) having too little coolant, as in a loss-of- coolant accident (LOCA). Both of these severe accidents are treated in detail in Chapter 28. We present a short introduction here.

9.7.1. Loss-of-Coolant Accident (LOCA)

The LOCA is a design-basis accident in light-water reactors. The postulated LOCA is initiated by a guillotine break in the primary piping, allowing coolant discharge into the containment building. Although the control rods shut down the reactor, power continues to be produced by the decay heat of the fission products, which amounts to approximately 8% of the full-power thermal output of the reactor (Chap. 28). For a 1000 MWe reactor the fission products produce ~ 240 MW of heat. In addition, thermal energy is stored in the fuel from the temperature gradients necessary to drive heat flow during normal operation. PCMI and cladding overheating by the combination of decay heat and stored energy can be avoided by water from the Emergency Core-Cooling System (ECCS).

The maximum allowable cladding temperature of 1205^{o}C was derived by following the severity of the accident as the temperature of the cladding. At this temperature, and in the presence of steam, cladding corrosion becomes a runaway reaction. If the temperature is kept below the 1205^{o}C limit the cladding can survive a LOCA. Thus it is necessary using Fuel-performance models to show with reasonable certainty that the cladding temperature remains below the limit for postulated LOCA accidents.

As the fuel temperature increases during a transient, fission gas release accelerates with a corresponding increase of the internal rod pressure. . Simultaneously the Zircaloy yield stress decreases (see Chapter 11) and the cladding yields balloons and may rupture (Sect. 28.4). .

Ballooning reduces the area for coolant flow in the fuel channel, which further enhances local overheating of the fuel rod. However, blockage and cladding rupture followed by release of fission products is not the worst potential outcome of a LOCA. I If the cladding remains at high temperature just prior to injection of cold water by the ECCS, cladding embrittlement can cause the cladding to shatter.

Ring compression tests were conducted to assess the acceleration of cladding corrosion from a high-temperature excursion during a LOCA and the accompanying reduction of post-quench ductility [9]. These results established that if the extent of oxidation from time-at-temperature remained below a certain level, cladding ductility would not be unduly compromised. High-temperature oxidation results in formation of ZrO_2 as well as increased oxygen absorption by the cladding. Consequently, a limit is established in terms of the *equivalent cladding reacted* (ECR), which is the fraction of the cladding that would be consumed if all the oxygen absorbed were used to form ZrO_2. It was found that if the ECR is kept below 17%, the cladding retains enough ductility to remain intact during the LOCA.

9.7.2. Reactivity-Initiated Accident (RIA)

Although reactivity initiated accidents (RIAs) are improbable (none has ever occurred in a commercial LWR), it is necessary to demonstrate (by calculation) that whatever the extent of fuel damage, a coolable geometry is maintained. RIAs are discussed in detail in Chap. 28. Operating limits were established by tests in which reactivity was suddenly inserted by the ejection (PWR) or drop (BWR) of a control rod. The ensuing increase in fission rate leads to an expansion of the fuel against the cladding (PCMI) which then can rupture. I If the failure is “severe” a loss of coolable geometry results. . The critical parameter is the total energy deposition during the transient. MacDonald and co-workers showed [10] that if the deposited enthalpy in the fuel was less than 180 cal/g (752 kJ/kg) no fuel failure occurred and if less than 280 cal/g (1170 kJ/kg) no fuel dispersal occurred. T It must then be demonstrated that reactivity insertions resulting in energy depositions higher than those values are extremely unlikely. Recent results have indicated that the above limits, which were derived for fresh fuel, may be lower for high-burnup fuel [11].

9.7.3 Stored Energy

One of the consequences of low fuel thermal conductivity is a large temperature gradient needed to drive the heat from the fuel to the coolant. An upshot is significant thermal energy stored in the fuel. This is one reason why cooling must continue following a loss-of-coolant accident. Otherwise, the temperature redistributes across the entire rod until the fuel and cladding temperatures equalize. This could cause the cladding temperature to rise above acceptable limits.

The stored energy per unit length of fuel rod is

$$E_{stored} = (\rho C_P)_F \int_0^{R_F} 2\pi r (T_F - T_S) dr = (\rho C_P)_F \frac{(LHR) R_F^2}{8 k_F} \tag{9.48}$$

for a parabolic temperature distribution (Eqs (9.10 and (9.11)).

The coolant needs to provide enough heat-transfer capability to remove at least this much thermal energy, in addition to the heat generated by fission product decay, before the fuel melts or the cladding ruptures.

Example 9. 6

A section of fuel rod is happily operating at LHR = 200 W/cm when the reactor is scrammed and the coolant flow drastically reduced. What h_{cool} (cladding outer diameter-to-coolant heat transfer coefficient) is required to prevent an increase in the mean cladding temperature to 1205 ^oC? For fuel-rod properties, see Table 9.1. Neglect decay heat and heat from cladding oxidation. Assume a constant fuel thermal conductivity of 0.03 W/cm-K. Ignore the thermal resistance of the gap. The fuel is 1 cm in diameter and the cladding is 0.1 cm thick.

The transient that follows is governed by:

$$\frac{\partial T_F}{\partial t} = \kappa_F \frac{1}{r} \frac{\partial}{\partial r} \left(r \frac{\partial T_F}{\partial r} \right) \tag{9.49}$$

Where $\kappa_F = k_F/(\rho C_P)_F$ is the fuel thermal diffusivity.

The initial condition is:

$$T_F(r,0) = \frac{LHR}{4\pi k_F} \left(1 - \frac{r^2}{R_F^2} + \frac{2k_F}{R_F h} \right) = 530 \left(1.6 - \frac{r^2}{R_F^2} \right) \tag{9.50}$$

The steady-state h_{cool} = 2.5 W/cm^2-K and k_C/δ_C = 1.7 W/cm^2-K, so from Eq (9.21) h = 1.0 W/cm^2-K.

$$\left(\frac{\partial T_F}{\partial r} \right)_{r=0} = 0 \qquad and \qquad T_F(R_F, t) = \bar{T}_C(t) \tag{9.51}$$

The average cladding temperature obeys:

$$\delta_C (\rho C_P)_C \frac{d\bar{T}_C}{dt} = -k_F \left(\frac{\partial T_F}{\partial r} \right)_{r=R_F} - h_{cool} (\bar{T}_C - T_{cool}) \tag{9.52}$$

The initial mean cladding temperature is obtained from:

$$\frac{LHR}{2\pi R_{CO}} = h_{cool}^{o}\left((\bar{T}_C)_0 - (T_{cool})_0\right) \tag{9.53}$$

Where the quantities on the right-hand side are pre-scram values.

Problem: how to calculate T_{cool} for t > 0? This involves the entire fuel rod below the elevation in question. If this can be prescribed as a function of time, the value of h_{cool} to keep $\overline{T}_C < 1200^{o}C$ can be calculated.

References

[1] R. Yang, O. Ozer, and H. Rosenbaum, "Current Challenges and Expectations of High Performance Fuel for the Millenium," in *Light Water Reactor Fuel Performance Meeting*, Park City, Utah, 2000.
[2] M. M. El-Wakil, *Nuclear Heat Transport*: American Nuclear Society, 1978.
[3] R. O. Meyer, "Fuel Behavior Under Abnormal Conditions," NRC2009.
[4] D. R. Olander, *Fundamental Aspects of Nuclear Reactor Fuel Elements*: ERDA, 1976.
[5] D. Baron, "Fuel thermal conductivity: a review of modeling available for UO2, (U,Gd)O2 and MOX," in *Proc. of seminar on Thermal Performance of High Burn-up LWR Fuel*, Cadarache, France, 1998, p. 99.
[6] IAEA, "Safety Margins of Operating Reactors," 2003.
[7] N. E. Todreas and M. S. Kazimi, *Nuclear Systems I, Thermal-hydraulic Fundamentals*: Taylor and Francis, 1990.
[8] J. S. Armijo, L. Coffin, and H. Rosenbaun, "Development of Zirconium–Barrier Fuel Cladding," in *11th International Symposium on Zr in the Nuclear Industry*, 1995, STP 1245, pp. 3-18.
[9] H. M. Chung and T. F. Kassner, "Embrittlement Criteria for Zircaloy Fuel Cladding Applicable to Accident Situations in Light-Water Reactors: Summary Report," NRC1980.
[10] P. E. MacDonald, S. L. Seiffert, Z. R. Martinson, R. K. McCardell, D. E. Owen, and S. K. Fukuda, "Assessment of light-water-reactor fuel damage during reactivity-initiated accident," *Nuclear Safety*, vol. 21, pp. 582-602, 1980.
[11] R. Meyer, R. K. McCardell, and H. H. Scott, "A Regulatory Assessment of Test Data for Reactivity Accidents," in *International Topical Meeting on Light Water Reactor Fuel Performance*, Portland, OR, 1997, pp. 729--744.

Problems

9.1. Verify that the burnup when expressed in MWd/kgU is equal to 877 x FIMA.

9.2 The temperature dependence of the thermal conductivity of UO_2 is given by Eq (9.35) with C = 0. From this, derive Eq (9.13). The rod linear power is LHR.

9.3 In calculating the temperature distribution in the cladding, the curvature is usually neglected and the geometry approximated as a slab.

(a) Derive the equation for the temperature difference between the inside and outside surfaces for cladding of thickness δ_c and inner cladding radius R_{cI} operating at linear power LHR. The cladding thermal conductivity is k_c.

(b) Show mathematically how the result of (a) reduces to for the case of thin cladding($\delta_c << R_{cI}$).

(c) The cladding of PWR fuel is 0.7 mm thick and 8 mm in diameter. What is the fractional error in the temperature difference due to the use of slab geometry?

9.4. Demonstrate equation (9.14)

9.5. Prove that the fractional thermal expansion of the outside diameter of a solid cylinder of radius R with thermal expansion coefficient α in a parabolic temperature distribution is $\alpha(\overline{T}_F - T_S)$, where $\overline{T}_F$ is the volume-averaged temperature of the solid.

9.6. Derive equation (9.35)

9.7 *Duplex fuel* consists of two radial zones with different enrichments of the uranium (see Fig. 16.4). Such pellets reduce the fuel centerline temperature below that of conventional uniformly-enriched fuel operating at the same linear power. In a particular fuel design, the center of the pellet to a radius r_i consists of natural uranium and the outer annulus $R_{FI}<r<R_F$ contains 4% enriched fuel. This fuel design is to be compared to conventional single-enrichment fuel containing 3.2% ^{235}U, neglecting neutron-flux depression in the pellet and assuming a temperature-independent fuel thermal conductivity.

(a) What is the value of R_{FI} that gives the same average power density in the duplex and homogeneous fuels?

(b) What is the ratio of the temperature difference between the fuel centerline and surface for the two designs at the same linear power?

9.8 Solutions to transient heat-conduction problems often are expressed in terms of a dimensionless time $\kappa t/d^2$ and a dimensionless position r/d, where $\kappa = k/\rho C_p$ is the thermal diffusivity, d is a characteristic dimension of the body, and t and r are time and position, respectively. The ratio d^2/κ is a *characteristic time* for the problem. When the imposed time scale of the transient is much longer than the characteristic time, the quasi-steady-state form of the heat conduction equation is sufficient for the analysis. If the transient

occurs in times shorter or comparable to the characteristic time, the full time-dependent heat conduction equation must be solved.

(a) A PWR is shut down from full power in 1/2 minute. Considering typical properties, which components of the fuel rod (fuel and cladding) can be treated by quasi-steady-state heat conduction during this transient?

(b) The first wall of a fusion reactor is a steel plate 1 cm thick. The back side of the wall is maintained at constant temperature by a coolant. The front face is suddenly exposed to a plasma disruption that increases the heat flux instantaneously. Approximately how long is required for the increased heat load on the front face be felt at the back face of the wall? The thermal conductivity, heat capacity, and density of the particular steel are 0.23 W/cm-K, 0.32 J/g-K, and 8.7 g/cm^3, respectively.

9.9 A fuel rod operates at a linear power P with a radial power density distribution $H(r)=H_o+\mathbf{a}r^2$, where H_o and **a** are constants. **a** is positive because the effect it describes is the neutron flux depression in the fuel pellet. What is the difference between the centerline-to-surface temperature difference for this rod compared to one operating at the same linear power but with a uniform radial power density distribution?

9.10 A fast reactor fuel pin operates at a linear power of 700 W/cm at an axial location where the coolant (liquid sodium) is 500^{o}C. Under these conditions, a central portion of the fuel is molten. The heat transfer properties of this fuel pin are:

$k_{gap}/\delta_{gap} = 0.5$ W/cm^2-K
$k_c/\delta_c = 9$ W/cm^2-K
$h_{cool} = 12$ W/cm^2-K
$k_{solid\ fuel} = 0.03$ W/cm-K
$k_{liquid\ fuel} = 0.05$ W/cm-K
$R_F = 0.35$ cm

(a) What is the fuel surface temperature?
(b) To what fractional radius is the fuel molten?
(c) What is the fuel centerline temperature?

9.11 A key safety limit in light-water reactors is the *stored energy* in the fuel. This is the thermal energy (relative to 25^{o}C) contained in the temperature distributions in the fuel pellet and in the cladding. In the event of a loss-of-coolant accident, flowing liquid water is replaced by stagnant steam, which acts as an insulating blanket over the fuel rod. Even though heat production by fission has been shut off, the original temperature profiles relax to a constant temperature that is the same in both fuel and cladding. This final temperature must not exceed a regulatory limit.

Before shutdown, the fuel operated at 500 W/cm linear power and the local water coolant temperature was 300^{o}C. The fuel pellet diameter is 1 cm and the cladding thickness is 1 mm. The fuel-cladding gap is closed, so the temperature drop across the gap is negligible. The external heat transfer coefficient in the water coolant is very large, so there is no temperature drop here either. Using the thermal properties given in the chapter,

(a) What are the T_o and T_S during operation?

(b) What is the final uniform fuel and cladding temperature after the adiabatic relaxation of the original distributions?